

KfK 3334
September 1982

Theoretical and Experimental Analysis of Fast Reactor Fuel Performance

K. R. Kummerer, D. Freund, H. Steiner
Institut für Material- und Festkörperforschung
Projekt Schneller Brüter

Kernforschungszentrum Karlsruhe

KERNFORSCHUNGSZENTRUM KARLSRUHE
Institut für Material- und Festkörperforschung
Projekt Schneller Brüter

KfK 3334

Theoretical and Experimental Analysis of Fast Reactor
Fuel Performance

K.R. Kummerer, D. Freund, H. Steiner

Vortrag gehalten auf dem Topical Meeting on Reactor Safety Aspects of
Fuel Behavior, August 2-6, 1981, Sun Valley, Idaho/USA

Reprint permitted by courtesy of the American Nuclear Society

Kernforschungszentrum Karlsruhe GmbH., Karlsruhe

Druck und Verbreitung:
Kernforschungszentrum Karlsruhe GmbH
Postfach 3640 · 7500 Karlsruhe 1
Bundesrepublik Deutschland

Copyright 1981 by the American Nuclear Society,
La Grange Park, Illinois, U.S.A.

ISSN 0303 - 4003

A b s t r a c t

Theoretical and Experimental Analysis of Fast Reactor Fuel Performance

In order to predict behavior, performance, and capability of prototypic fuel pins a standard operational scheme for the SNR-300 fast breeder reactor is established considering besides normal operation unscheduled power changes and shutdowns.

The behavior during the whole lifetime is calculated using the updated SATURN codes and - for special conditions as power transients and skewed fuel rod power - the new TRANSIENT and TEXDIF codes. The results of these calculations are compared to experimental findings.

It is demonstrated that the level of modeling and the knowledge of material properties under irradiation are sufficient for a quantitative description of the fuel pin performance under the above mentioned conditions.

Z u s a m m e n f a s s u n g

Theoretische und experimentelle Analyse des Verhaltens von Schnell- brüterbrennstäben

Für die Untersuchung des technologischen Verhaltens und des Betriebspotentials prototypischer Brennstäbe wird für den SNR-300 ein standardisiertes Betriebssystem aufgestellt, welches außer bestimmungsgemäßem Normalbetrieb auch nicht geplante Reaktorabschaltungen und Leistungsänderungen enthält. Auf dieser wirklichkeitsnahen Grundlage wird das Stabverhalten berechnet mit Hilfe der aktualisierten SATURN-Rechenprogramme und - für spezielle Bedingungen wie Leistungstransienten und Schiefplast über den Stabquerschnitt - mit Hilfe der neuen Programme TRANSIENT und TEXDIF. Die Ergebnisse dieser rechnerischen Untersuchungen werden mit experimentellen Befunden verglichen.

Es kann gezeigt werden, daß der erreichte Stand in der modellmäßigen Beschreibung sowie die Kenntnisse der Materialeigenschaften unter Bestrahlung eine weitgehend zutreffende Darstellung der Wirklichkeit ermöglichen.

C o n t e n t s :

Introduction
Standard Operational Scheme
Startup Period and Short Term Behavior
Status in the 1 at % Burnup Region
Power Ramping
Longterm Features
Special Aspects
Conclusions

References
Fig. 1 - 19

INTRODUCTION

The subject of analyses is the oxide fuel pin according to the Mark-Ia and Mark-II design of the prototype fast reactor SNR-300¹. The general design and operational data are listed in Table I.

In the course of the development of such a fuel pin design, a major irradiation program is carried out². The experimental work includes steady state irradiations up to high burnup as well as transient tests under realistic conditions. The evaluation of these experiments is accompanied by fuel pin modeling calculations using adequately adapted computer codes.

In this paper we demonstrate the comparison between irradiation experience and calculated results for different periods and aspects within the lifetime of a fuel pin.

STANDARD OPERATIONAL SCHEME

An idealized operation scheme for the fuel elements in a power reactor is composed of large operational cycles which are interrupted by shutdown periods for refueling. For a fast power reactor like the prototype SNR-300 the general standard scheme may last about 1.5 years, divided into 3 cycles

Table I Design and Operational Data of SNR-300 Fuel Pins

		S N R - 300	
		MARK-Ia	MARK II
Fuel Pin	Diameter (mm)	6.0	7.6
	Total Length (mm)	2475	2475
Fuel	Material	UO ₂ -PuO ₂	
	Length (mm)	950	950
	Diameter	5.09	6.40
	Bulk density (% T.D.)	86.5	95.0
	Smear density (% T.D.)	80.0	88.0
Cladding	Material	1.4970	1.4970
	Wall thickness (mm)	0.38	0.50
Linear rod power, max ^{x)}	(W/cm)	355/500	450/600
Cladding temperature, max. x)	(°C)	620/685	620/685
Burnup, local max.	(MWD/kgM)	85	85
Pins per subassembly		169	127
Pitch-to-diameter ratio		1.32	1.17
Spacer type		Grid	Grid

x) nominal condition/hot spot condition

of 24 weeks each with a 4 weeks shutdown time in between, see Fig. 1. The final burnup at the nominal local maximum is assumed to be 85 000 MWD/tM or roughly 9 at %.

At the scheduled base load operation of the power plant there is a non-steady-operation substructure in the real course of reactor power due to unscheduled events like reactor scrams, smooth or abrupt power changes including intermediate shutdowns followed by startup periods.

A regular startup operation from zero power to 100 % full load lasts about 30 hours including a holdup time at - say - 85 % of full power for relocation and restructuring of the fresh fuel, see the startup scheme in Fig. 2. For following startups the holdup time may be shorter and has to be orientated on avoiding severe fuel clad mechanical interaction.

A regular shut down diagram is sketched in Fig. 3, lasting e.g. 3.5 hours.

In a reactor scram the power is reduced to about 10 % within a very short time. After this sharp power change the pattern of further reduction down to zero is somewhat smoother. In Fig. 4 a typical (and simplified) scram diagram is outlined.

As a more general background the lifetime behavior of a fuel pin is calculated using the computer code SATURN 2, which was newly updated in the relevant material properties and phenomena³. This lifetime calculation does not take into account power changes and interruptions, but assumes a steady state operation up to high burnup. In these calculations all the restructuring and redistribution processes in the fuel as e.g. pore migration, central void formation, fuel cracking, gap closure, migration of plutonium and oxygen, as well as fission gas behavior have been taken into account.

The results of the calculations can be summarized as follows:

- At begin of life with a linear rod power of 450 W/cm, the fuel central temperature has its maximum at 2570 °C, corresponding to a gap heat transfer coefficient of 0.8 W/cm²·K at a radial gap width of 25 μm.
- Within about 48 hours this temperature decreases to 2400 °C. During this time the main restructuring takes place, leading to a central void of about 1.2 mm diameter mean value. At this stage equilibrium in porosity and plutonium redistribution is nearly achieved. A typical set of calculational results is shown in Fig. 5.
- Gap closure occurs after about 550 hours, leading to a further temperature decrease to about 2200 °C.
- At end of life a fission gas pressure buildup of 60 bars corresponding to a release rate of 80 % has been calculated.

In the following chapters experimental findings are compared to theoretical results for different experiments at various time steps.

STARTUP PERIOD AND SHORT TERM BEHAVIOR

In order to get experimental proof for the short term behavior within the startup period, the radial restructuring is evaluated by the post irradiation examination after short term exposure. These experimental results are compared to theoretical calculations of the structure changes during - say - the first 250 hours.

In the so-called DUELL series - startup experiments in the HFR reactor in Petten/Netherlands⁴ - the fuel pins are mounted in a pool side facility which can be moved towards the reactor core. In these experiments the fuel restructuring shows a marked radial eccentricity due to a steep flux gradient. Therefore, a special fuel modeling program was developed - the code TEXDIF-P⁵ - which solves the equation of two-dimensional heat conduction using finite differences method. With this type of modeling work the asymmetric temperature distribution and the resulting eccentric structure can be recalculated. Implementing the relevant subprogram of the SATURN modeling system allows the dynamic two-dimensional calculation of the radial pore migration. Independent of this, the program includes an option for the determination of the limit of pore migration zone via a relation covering the minimum pore migration path⁶.

The special aspect of eccentricity is treated further below. Independent of the steeply skewed rod power, the diameter of the central channel is a very characteristic feature formed in the startup period. In Fig. 6 a pin irradiation out of the DUELL experiments is evaluated in this respect. The startup power course was similar to the scheme in figure 2 with an extended period at the 85 % power level. (The final rod power of 530 W/cm in the thermal flux of the HFR corresponds to about 450 W/cm in a fast flux.) According to the calculations, the central channel is formed at the power level of 85 % and reaches its maximum after the power rise to 100 %. The experimental values are quantitatively consistent to these theoretical findings.

A quite detailed information on fuel restructuring in the startup period was produced by an irradiation series in the test reactor FR 2 in Karlsruhe. This series - called FR 2-Loop 3 - comprised the irradiation for two different fuel densities; a couple of identical specimens delivered a good insight into the formation and radial growth of the restructuring regions⁷. In Fig. 7 central void formation and columnar grain zone results

are presented. The theoretical curves - produced by the code SATURN 1 - are in good agreement to the experimental results. As Fig. 8 shows, there is only a slight dependence on linear rod power, especially for the central void diameter.

STATUS IN THE 1 AT % BURNUP REGION

After irradiation up to about 1 at % burnup, in addition to the startup restructuring of the fuel some of the longterm properties come into the picture. The redistribution of the fuel is more or less completed. The experimental values out of an irradiation in the PHENIX reactor in France correspond with calculational results produced by the SATURN 2 code, see Fig. 9. The radial Pu-segregation due to temperature and oxygen/metal ratio gradients becomes relevant, Fig. 10. The calculated plutonium contents in the innermost zone are higher than measured. This can be attributed to a numerical treatment allowing a maximum porosity of about 50 % near the central void, which enhances Pu-migration.

Due to the beginning of fuel swelling the radial gap width between fuel and clad is reduced. Taking into account the counteraction of fuel densification, the theoretical results in Fig. 11 are typical for the low burnup region. The measured residual gap value for 425 W/cm is somewhat higher than the calculated one. This may be caused by a too low densification rate in the model.

An example for radial pore distribution is shown in Fig. 12, demonstrating some results of the Mol-8D irradiation⁸ in the BR 2 reactor in Belgium. At a burnup status of 1.8 at % the experimental results correspond satisfactorily to the SATURN calculations.

POWER RAMPING

The decisive and most interesting feature at power ramping of fuel pins is the mechanical interaction between fuel and clad. While at steady state operation of oxide fuel pins only minor mechanical interactions are to be expected, at power transients the forces may impair the geometry and integrity of the clad. We distinguish in this context slow power ramps (power changes ≤ 10 W/cm \cdot min) and fast power ramps (≥ 50 W/cm \cdot min).

Experimental experience for slow power ramping was gained in the last years primarily in thermal reactors^{9,10}. As under these circumstances swelling and irradiation creep in the cladding is suppressed, an experimental verification of fuel clad mechanical interaction becomes possible. In such experiments clad strains of up to 1.8 % were ascertained which cannot be attributed to fission gas pressure. Furthermore, different fuel pins of the same type, loaded into identical rigs and having reached nearly the same burnup, differed totally in the amount of cladding strain. A thorough analysis revealed the decisive role of the detailed power history experienced by each single fuel pin in course of irradiation. The key for the explanation of the differing results was the individual character and amount of unscheduled power changes due to real reactor operation. The extent of cladding strain can be correlated to the total amount of positive power changes ("power humps") at the beginning of each reactor cycle. In Fig. 13 this correlation is demonstrated for fuel pins of two different experimental series in the FR 2^{10,11}.

For an assessment of the clad load due to such power ramping, the amount of power increase and the increase rate as well as the level and the duration of the preceding reduced power are of greatest importance¹². Furthermore, there is a limit for the increase rate below which the resulting stresses remain within the elastic region of the clad material. This increase rate limit was found to be dependent on the initial rod power and the amount of power increase¹³. Consequently, at slow power ramping, rod power changes up to 70 W/cm at constant cladding temperature are sustained by the cladding without plastic deformation. Very low increase rates, e.g. 0.5 W/cm·min, allow quite large total increases under all circumstances.

There are new experiments being prepared - the so-called KAKADU series in the HFR reactor in the Netherlands⁴ - where the response of fuel pins on power cycling between 65 and 100 % of nominal full power will be studied with two values of increase rates (0.5 and 6 W/cm·min).

For the discussion of fast power ramps, calculations using the newly established code TRANSIENT¹⁴ were carried out. One realizes that the brittle to ductile transition temperature in the fuel, especially its dependence on the strain rate, is important. It strongly influences the width of the mechanically strong zone in the fuel pellet. For our calculations, we used the correlations reported by Roberts and Wrona¹⁵ and extrapolated them to higher strain rates. The results in Fig. 14 for a fast power increase show the contact pressure buildup. In this case, it was assumed that the fuel cracks caused by the preceding power reduction were completely healed out. It is important to notice that the load on the cladding is also dependent on the amount and distribution of the crack volume in the fuel pellet, this crack volume being a function of the preceding power history. The plastic strain in this calculational example was about 0.02 % in the maximum power region, while higher values of about 0,17 % were reached at the lower part of the fuel pin.

LONGTERM FEATURES

While the overall fuel structure at steady state irradiations is not very much changed in the course of further burnup above 1 or 2 at %, there are some characteristic longterm features like fission product accumulation, thermal conductivity etc. In this context we want to demonstrate and evaluate the results of unique in-pile measurements of central fuel temperature and fission gas pressure buildup.

The long term fuel temperature slope has been thoroughly investigated in the experiment series Mol-8D⁸ in the BR 2. Twelve fuel pins with fuel central thermocouples have been irradiated to burnups between 2 and 9 at %. Accompanying real case calculations with SATURN show that calculated and measured temperatures correspond well within small error limits. In Fig. 15 a simplified diagram of fuel centerline temperatures up to about 5 at % burnup is depicted. The calculated results - based on real case irradiation conditions - are in good agreement to the thermocouple readings. The evaluation of in-pile experiments up to even higher burnup is in preparation.

Another long term aspect of high interest is the fission gas release. In the experiment series Mol-8C⁹, the measurement of fission gas pressure buildup has been carried out continuously up to 10 at %, Fig. 16. In spite of a very complex irradiation history with 50 to 60 thermal cycles of the BR 2, preliminary real case calculations show that the results coincide well with measured values up to high burnup.

SPECIAL ASPECTS

In addition to the main performance parameters outlined in the preceding chapters, there are a lot of aspects and conditions which are not taken into account at a routine design and evaluation study. But the unscheduled off-normal operation case is to be considered as realistic as the normal operation, particularly in safety evaluations. We want to draw attention to three special aspects, namely

- the linear rod power leading to central fuel melting,
- the radial dependence of fission gas retention, and
- the fuel pin behavior under radially asymmetric conditions.

In the FR 2-Loop 3 irradiation series⁷ some fuel pin samples have been irradiated at various rod powers leading to fuel melting. In the considered fuel pins, melting occurred at rod powers above 570 W/cm for 85 % fuel density and above 650 W/cm for 90 % of the theoretical fuel density, being in good accordance with calculations. In all the cases no pin failed even at more than 25 % melting area.

The retention of fission gas in the fuel is highly dependent on temperature and fuel structure. In Fig. 17 a calculation with the code TRANSIENT demonstrates the radial dependence for a typical fuel region of 450 W/cm rod power and 1 at % burnup. Experimental findings¹⁶ on a fuel with 2 at % burnup, comparable to the calculated case, show in Fig. 17 a very similar fission gas distribution, with, however, a somewhat sharper decrease towards the fuel center.

Radially asymmetric conditions may exist in a fuel pin located at the skewed power distribution near control elements or in a pin with a large as-fabricated gap size with eccentric position of the pellet. In order to evaluate the effects and consequences, mainly in terms of asymmetric restructuring and heat transfer, the code TEXDIF-P⁵ treats the phenomena in a two-dimensional manner. As already mentioned, the DUELL experiments are an example for such asymmetric power load. As is demonstrated in Fig. 18, the post irradiation examination revealed a marked asymmetric fuel restructuring. The TEXDIF-P calculations could reproduce size and location of the central void as well as the boundary of the pore migration zone in a satisfying manner. It is reasonable to assume that - in the first days of irradiation - the developing and growing central void is asymmetrically shifted. This feature corresponds to a further TEXDIF-P calculation in Fig. 19, where the contour of the void at consecutive irradiation times is sketched. All these results concerning fuel restructuring under asymmetric load confirm the reliability of the respective models used also in the SATURN codes.

CONCLUSIONS

During a standard operation scheme, fast reactor fuel pins undergo various temperature and load changes, which have to be analysed thoroughly to guarantee safe operation. Besides a widespread experimental program, modeling activities led to computer programs being able to describe fuel pin behavior under different operation conditions.

From begin of life up to high burnups, experimental results like fuel restructuring and material redistributions, temperature slope and fission gas behavior have been compared with modeling predictions. The results of all these calculations show that modeling as well as the actual knowledge of material data allow a quite quantitative description of fuel and fuel

pin types. The results indicate that the extrapolation of material properties is admissible in between certain ranges. Discrepancies, however, show that the interdependence of arising phenomena should thoroughly be analyzed to avoid misleading interpretation.

REFERENCES

1. K. Kummerer, "General Characteristics of Fast Reactor Fuel Pins", Proc. European Nucl. Conf. Paris, Vol. 3, 440 (1975)
2. K. Kummerer, "The German Oxide Fuel Pin Irradiation Test Experience for Fast Reactors", Proc. Internat. Conf. on Fast Breeder Reactor Fuel Performance Monterey, 29 (1979)
3. H. Elbel and J. Lopez-Jimenez, "Ein Beitrag zur Analyse des thermischen Verhaltens von Schnellbrüter-Brennstäben mit UO_2 - PuO_2 -Brennstoff", Rep. KfK 2216, Kernforschungszentrum Karlsruhe (1975)
4. D. Geithoff et al., "Operational Transient Test Irradiations of FBR Fuel", this conference
5. H. Steiner and H. Elbel, "Die Berechnung von Temperaturasymmetrien in gekapselten Brennstäben mit dem Rechenprogramm TEXDIF-P", Rep. KfK 2961, Kernforschungszentrum Karlsruhe (1980)
6. D.R. Olander, "Fundamental Aspects of Nuclear Reactor Fuel Elements", ERDA-Report TID-26711-P1, 275 (1976)
7. H. Fiedler and D. Freund, unpublished (1976)
8. H.J. Ritzhaupt-Kleissl and M. Heck, "Brennstabbestrahlungsexperiment Mol-8D, Messung der Brennstoffzentraltemperatur und modellmäßige Auswertung", KfK-Report in preparation
9. P. Weimar, H. Steiner and H. van den Boorn, "BR 2-Kapsel-Versuchsgruppe Mol-8C, zerstörungsfreie Nachuntersuchung", Rep. KfK 2306, Kernforschungszentrum Karlsruhe (1976)
10. P. Weimar, D. Freund and H. Steiner, "FR 2-Kapselversuchsgruppe 5b. Auslegung, Bestrahlung und Nachuntersuchung der UO_2 / PuO_2 Brennstabprüflinge", Rep. KfK 2222, Kernforschungszentrum Karlsruhe (1976)
11. H. Steiner, unpublished (1975)
12. W. Dienst et al., "Fuel Cladding Mechanical Interaction in Fast Breeder Fuel Pins, Observations and Analysis", Journ. Nucl. Mat., 91, 73 (1980)
13. I. Müller-Lyda, "Untersuchungen zur mechanischen Wechselwirkung zwischen Brennstoff und Hüllrohr in Brennstäben von Schnellen Brutreaktoren", Rep. KfK 3012, Kernforschungszentrum Karlsruhe (1980)

14. H. Steiner and I. Müller-Lyda, "Das Rechenprogramm TRANSIENT zur Berechnung transienter Brennstabbelastungen", KfK-Report in preparation
15. J.T. Roberts and B.J. Wrona, "Nature of Brittle-to-Ductile Transition in UO₂-20 wt % PuO₂ Nuclear Fuel", Journ. Nucl. Mat., 41, 23 (1971)
16. H. Kleykamp, personal communication (1981)

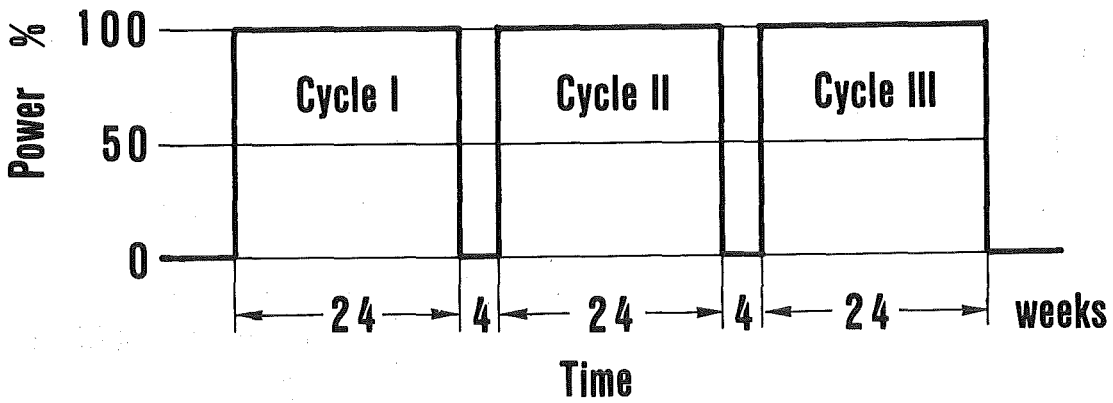
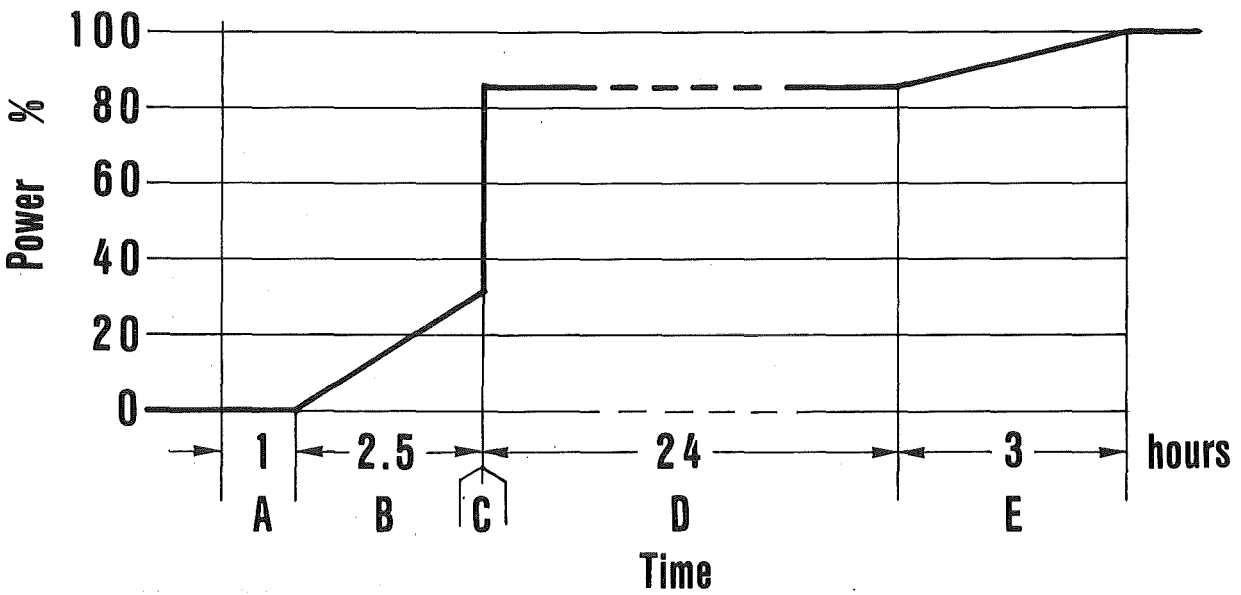
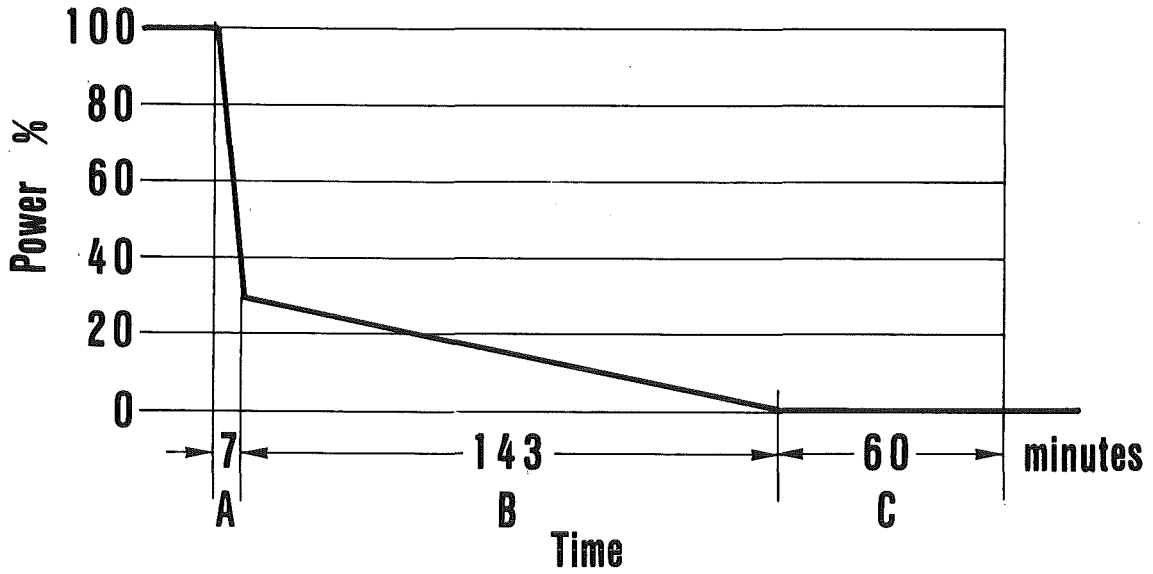


Fig. 1 General Standard Operation Scheme



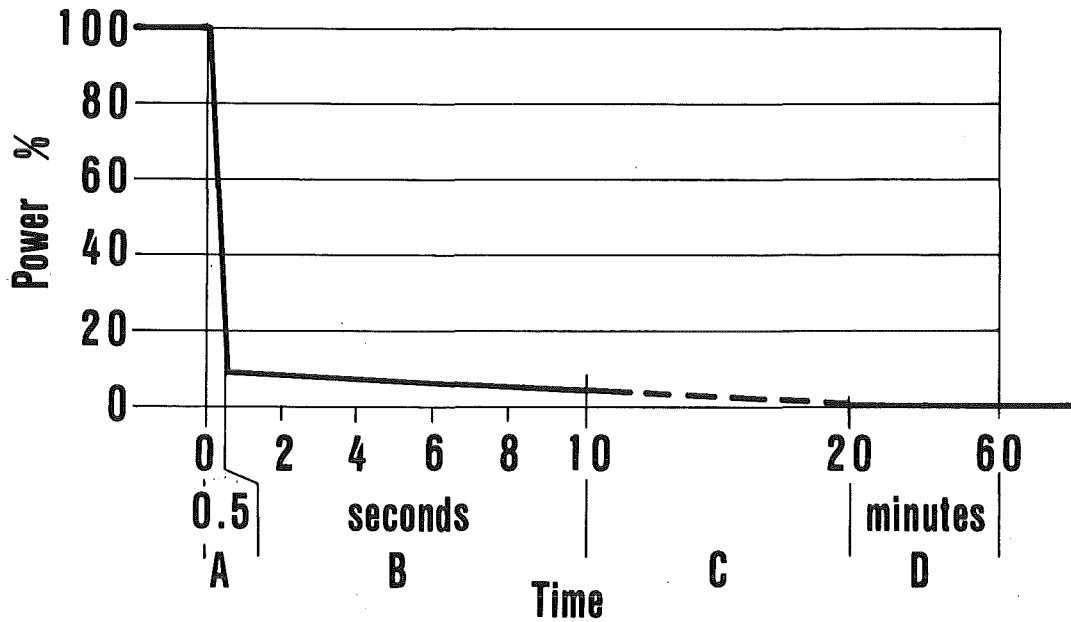
Section A: 0 → 1% in 1 h
Section B: 1 → 30% in 144 minutes (ca. 0,2% / min)
Section C: 30% → 85% in 6 minutes (ca. 10% / min)
Section D: 24 hours holdup at 85%
Section E: 85% → 100% in 3 hours (5% / h)

Fig. 2 Startup Operation Scheme



Section A: 100% → 30% in 7 minutes
Section B: 30% → 1% in 143 minutes
Section C: 1% → 0 in 60 minutes

Fig. 3 Shutdown Operation Scheme



Section A: 100% → 10% in 0.5 seconds
Section B: 10% → 5% in ca. 10 seconds
Section C: 5% → 1% in ca. 20 minutes
Section D: 1% → 0 in 40 minutes

Fig. 4 Power Reduction at Reactor Scram

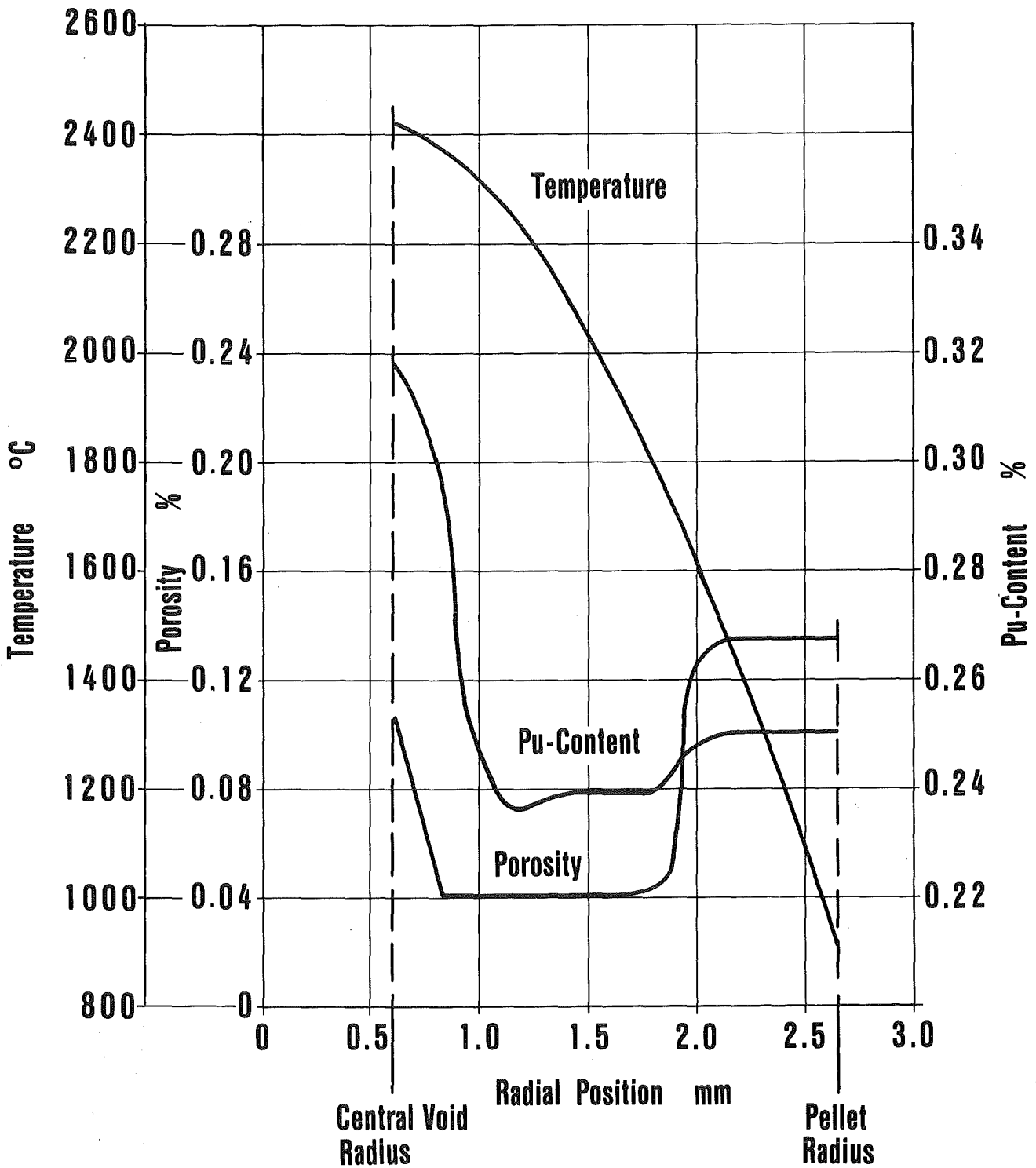


Fig. 5 Radial Restructuring and Redistribution of Fuel at 450 W/cm in Equilibrium Stage

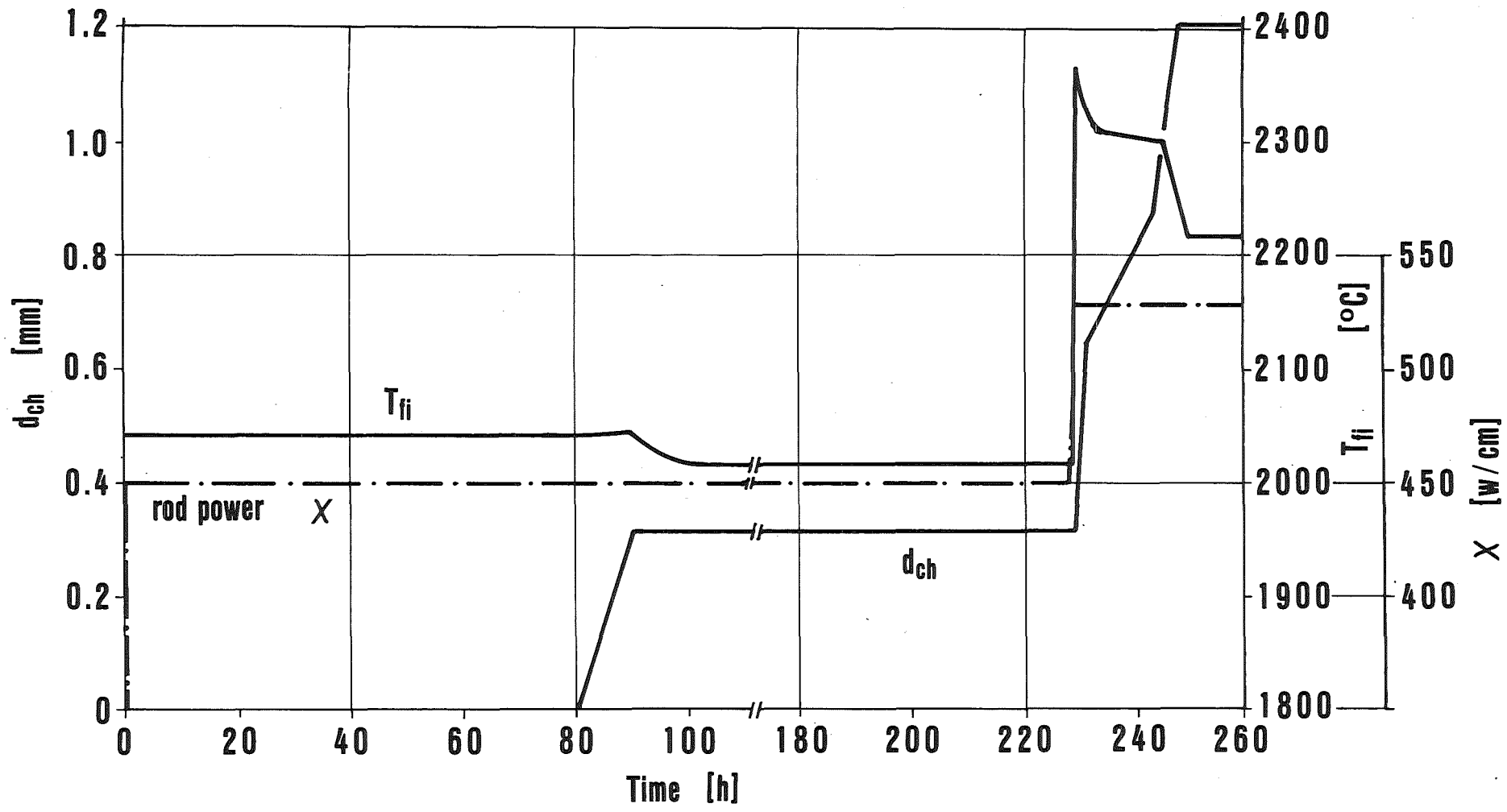


Fig. 6 Central Temperature (T_{fi}) and Central Channel Diameter (d_{ch}) in a Fuel Pin During the Startup Period

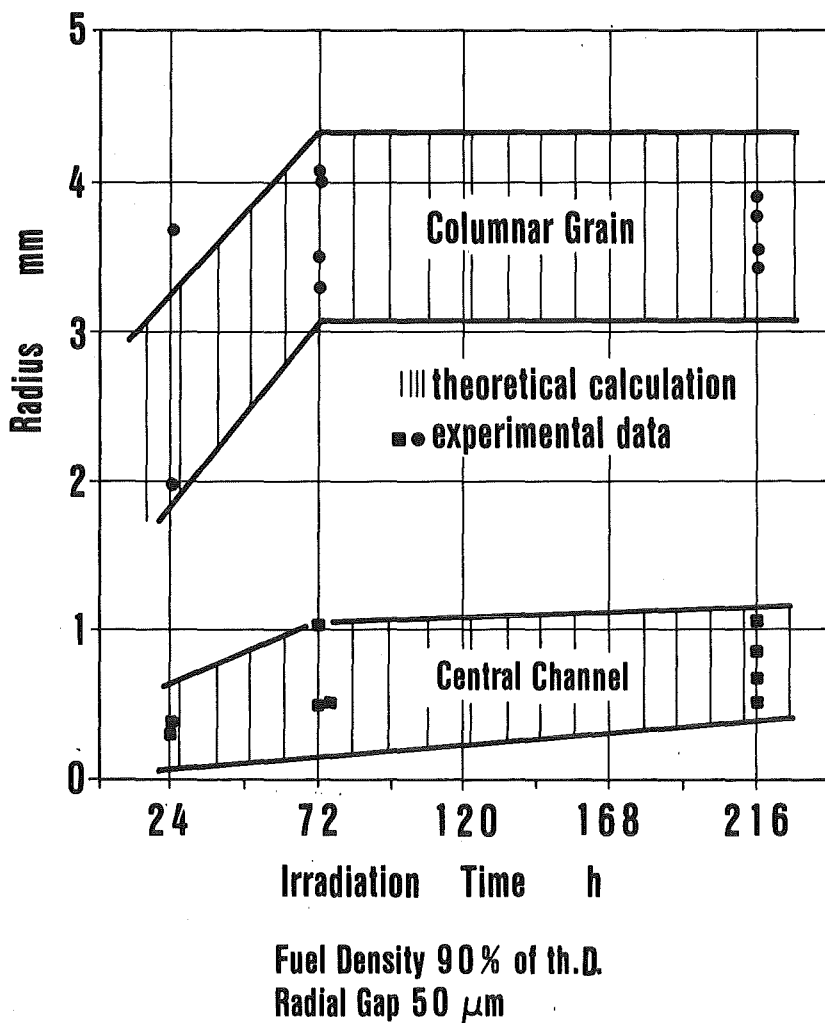


Fig. 7 Central Channel and Columnar Grain Growth in the Initial Period of Irradiation at 600 W/cm

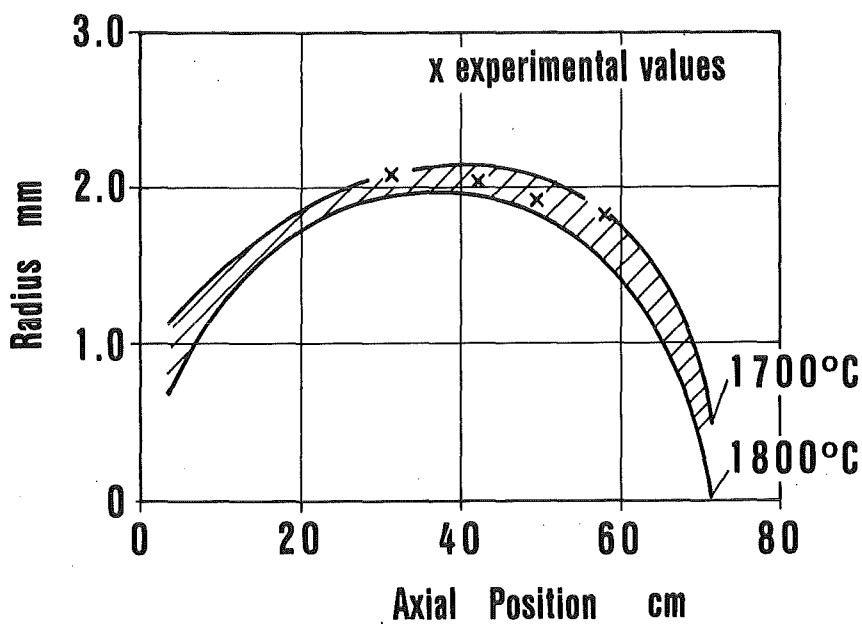
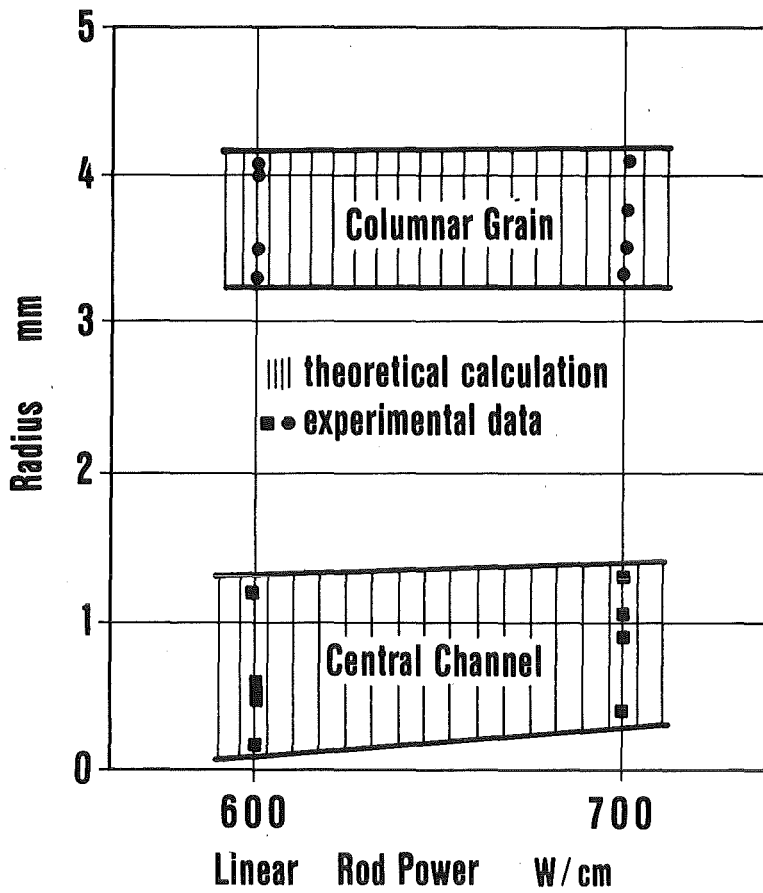


Fig. 9 Columnar Grain Region after 1 at % Burnup



Fuel Density 90% of th.D.
Radial Gap 50 μ m

Fig. 8 Restructuring after 72 hours of Irradiation

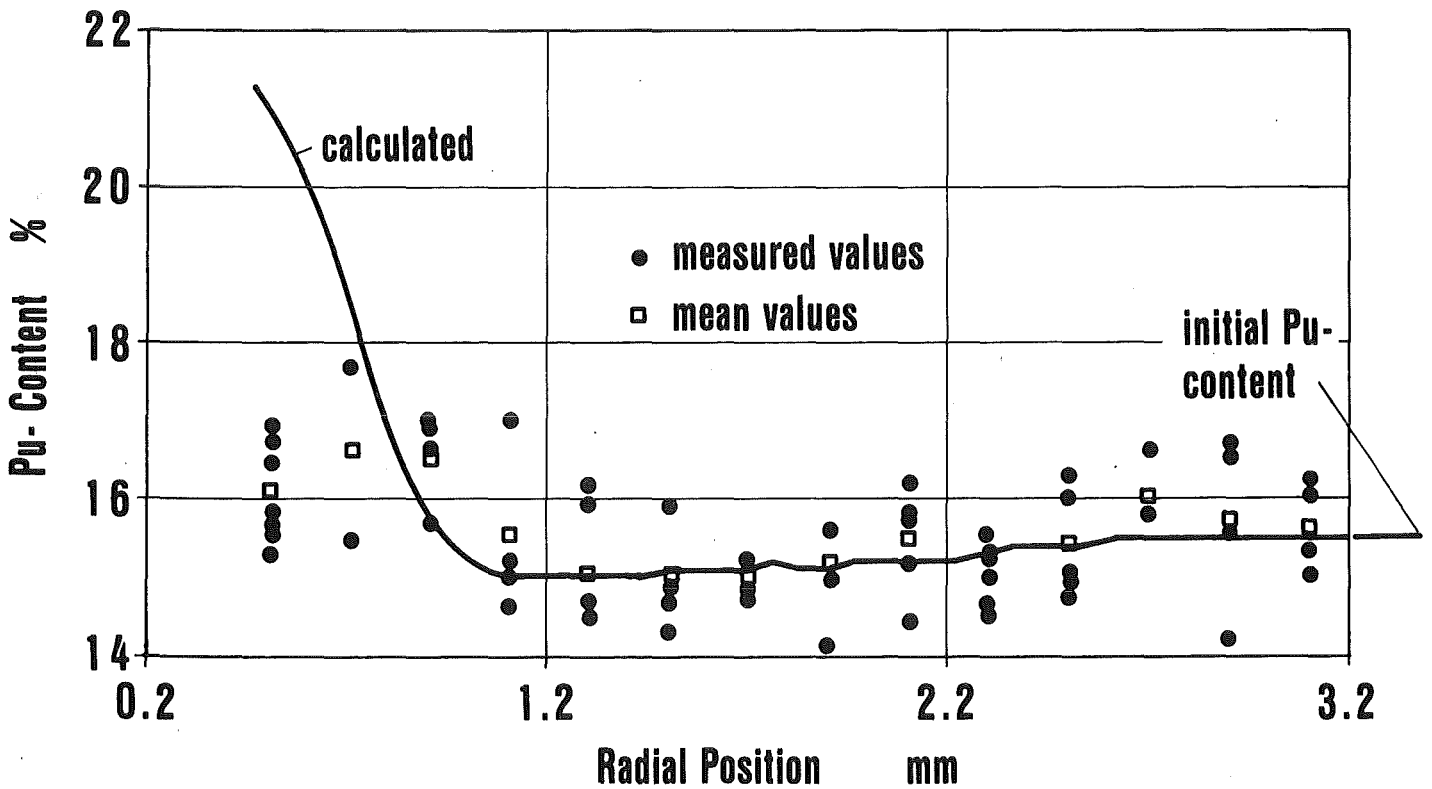
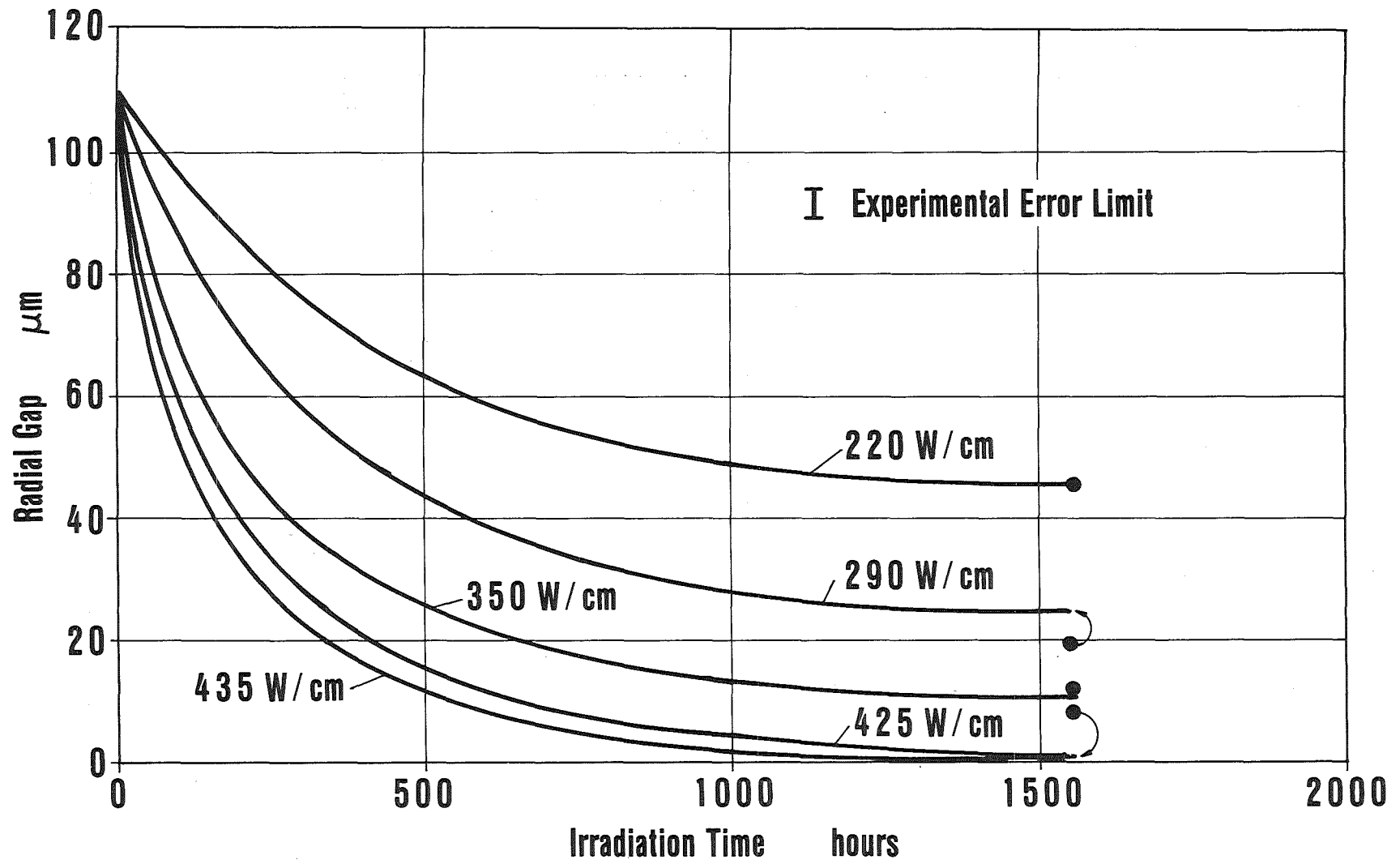


Fig. 10 Plutonium Segregation after 1 at % Burnup



Straight Lines: Calculations with SATURN 2

● Experimental Values

Fig. 11 Time Dependent Radial Gap Width

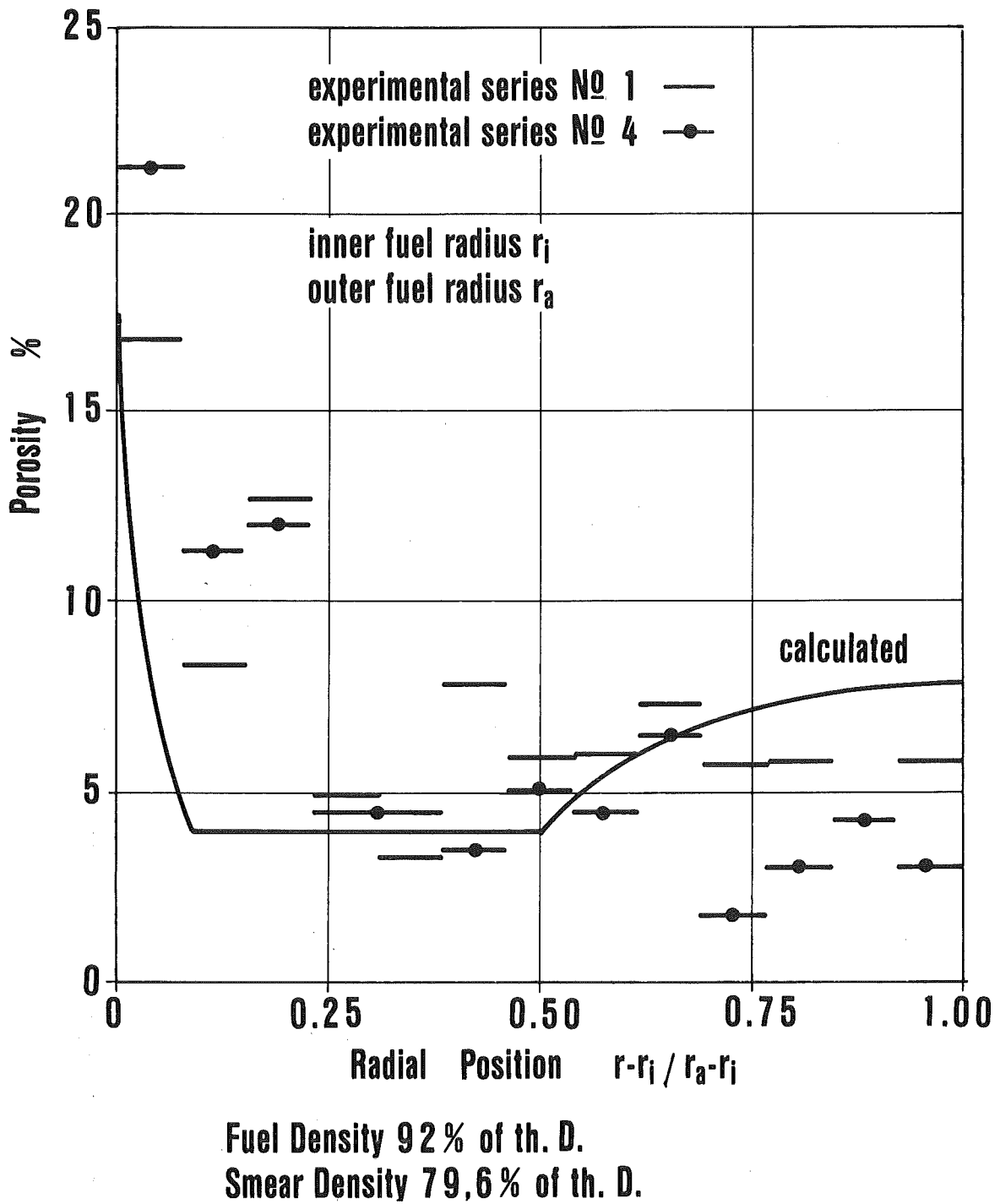


Fig. 12 Radial Pore Distribution after 1.8 at % Burnup

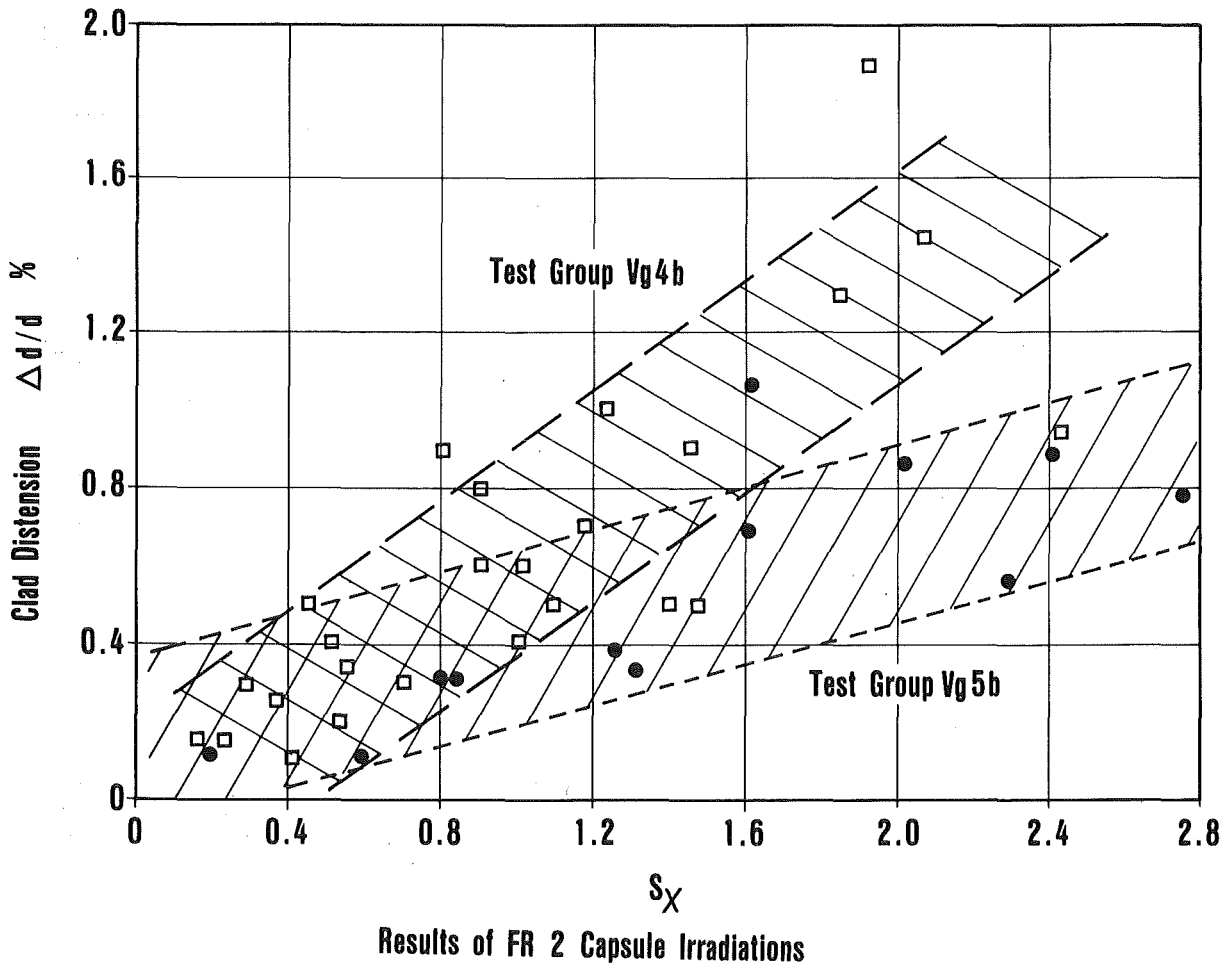


Fig. 13 Clad Distensions of Fuel Pins Versus the Sum S_x of Normalized Positive Power Changes

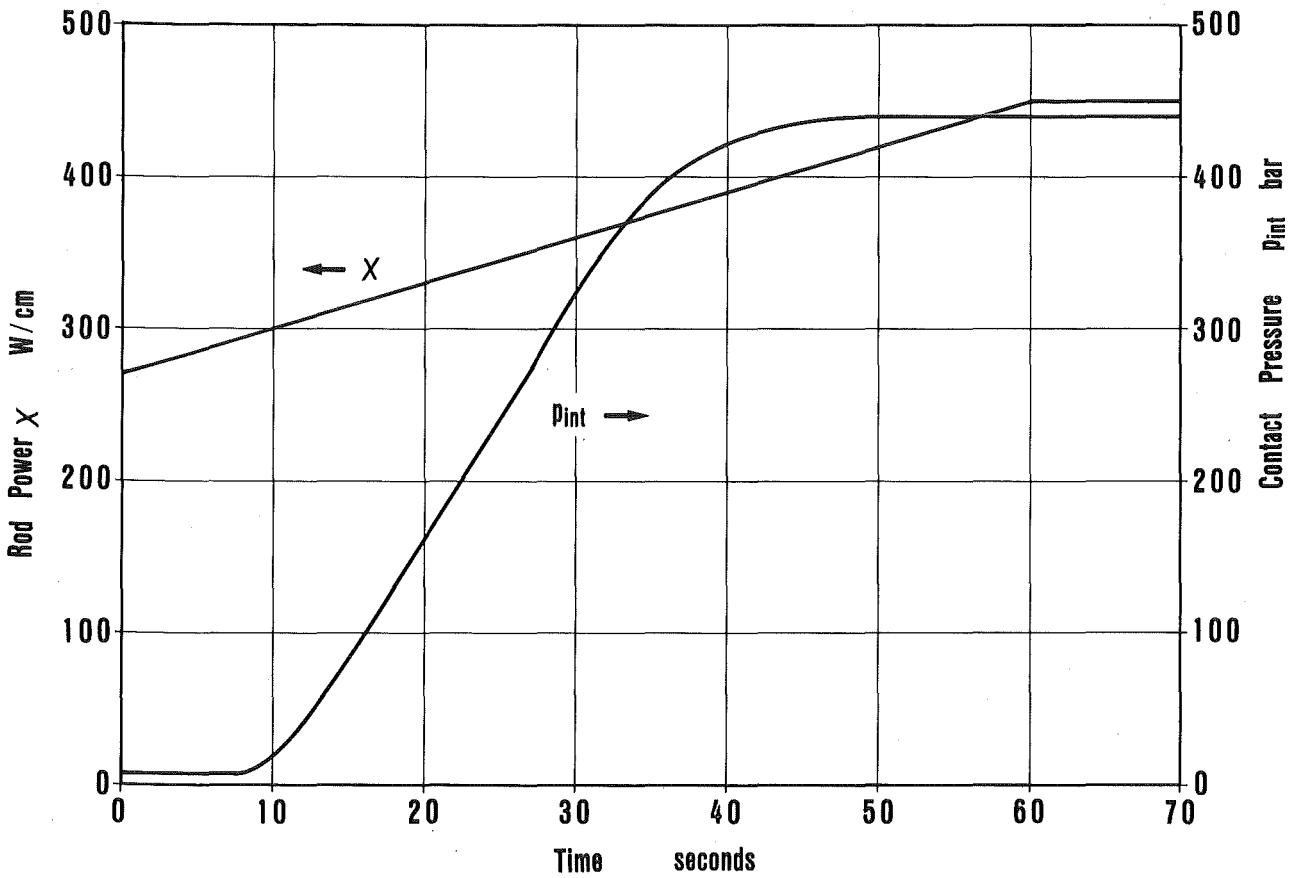


Fig. 14 Contact Pressure during a Fast Power Ramp, Calculational Results

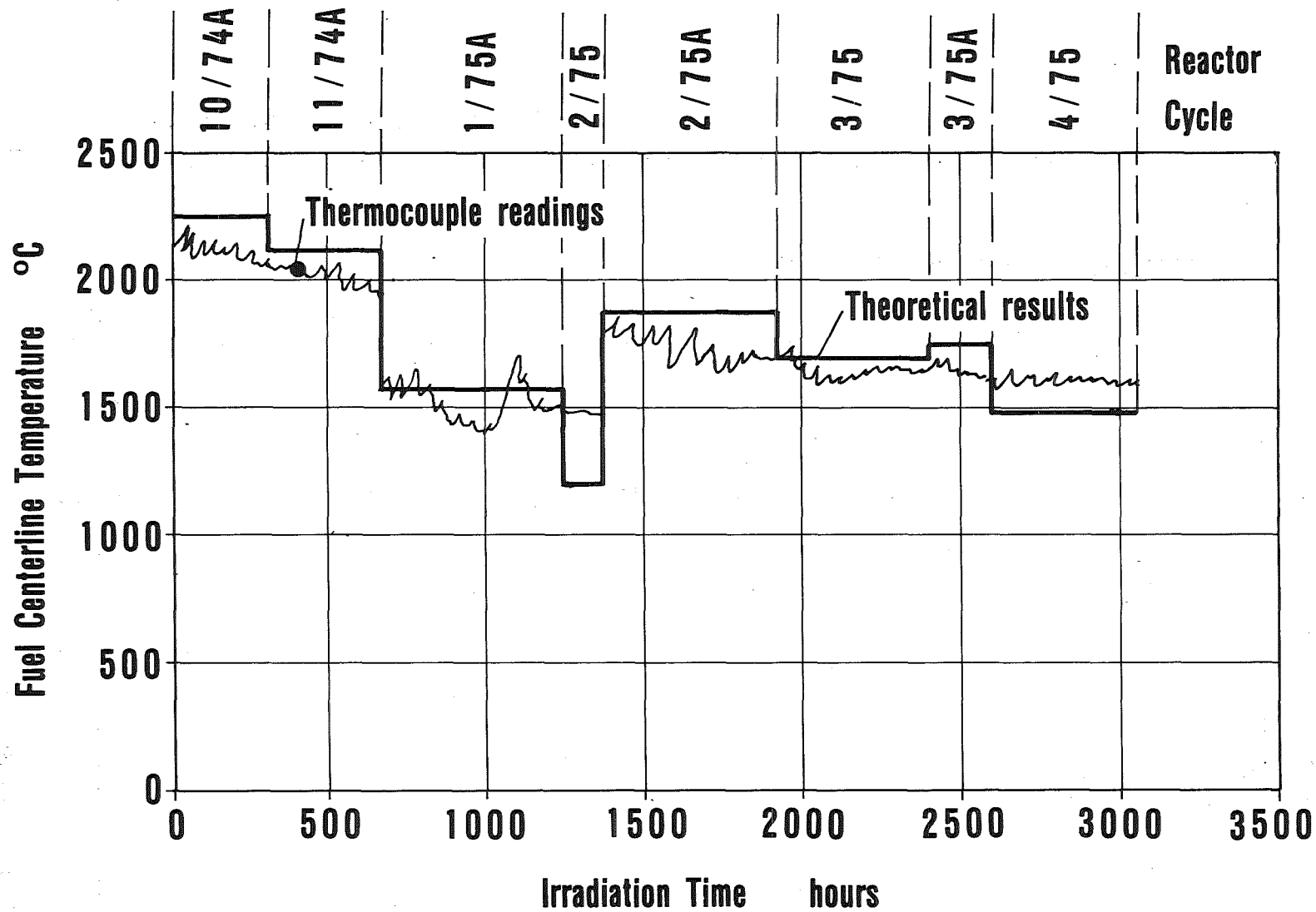


Fig. 15 Central Temperature in a Fuel Pin under Irradiation: Comparison between Experimental and Calculated Values

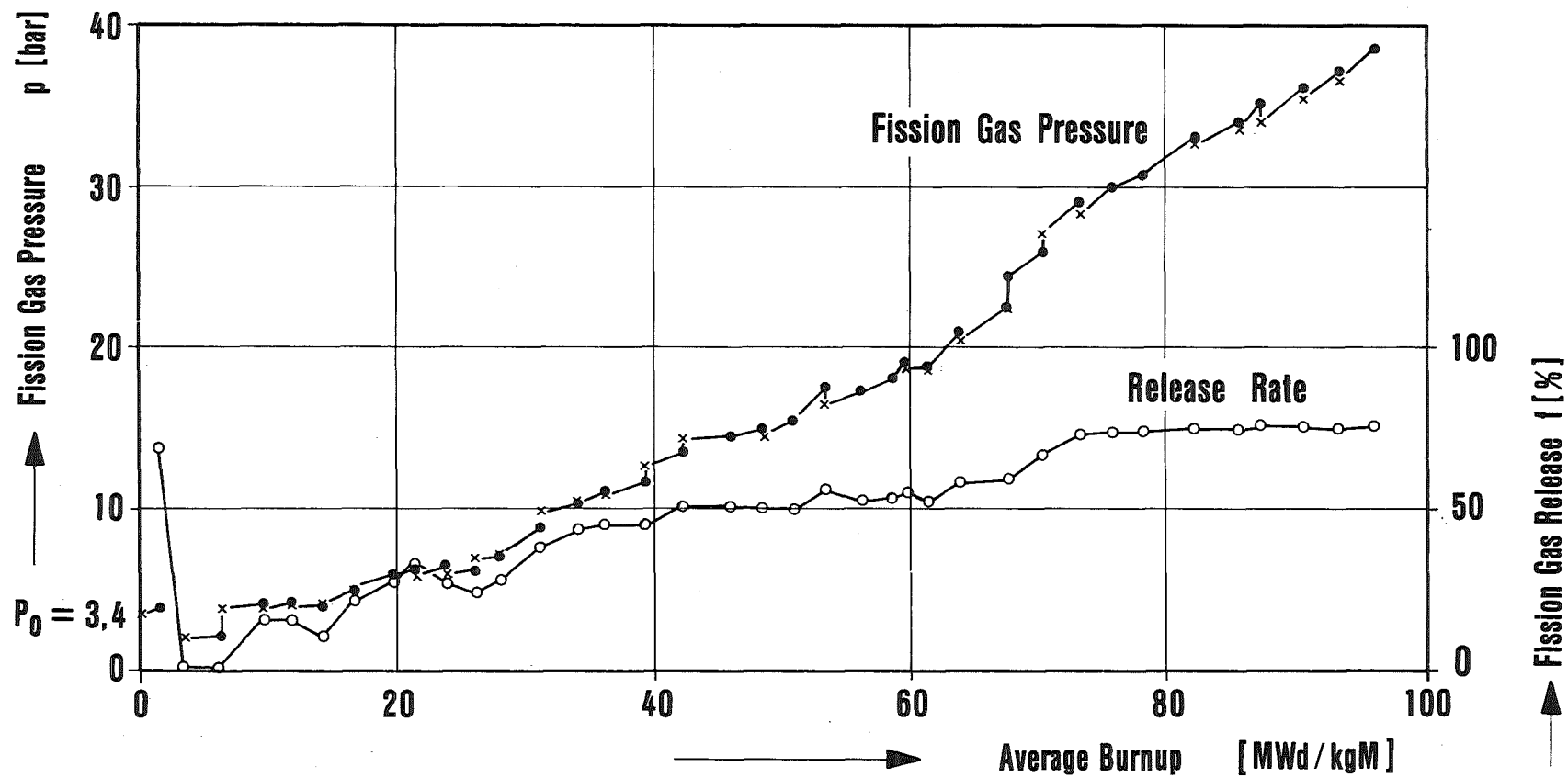
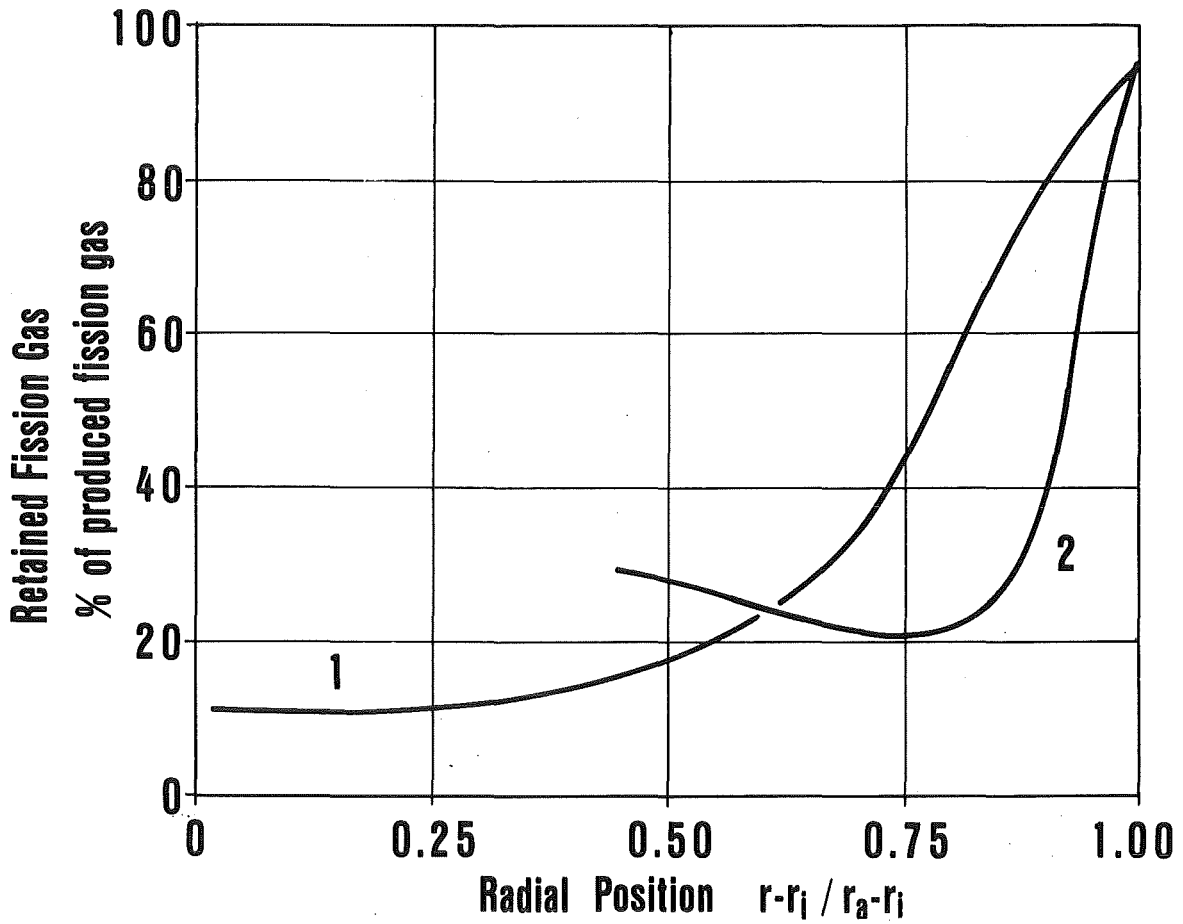
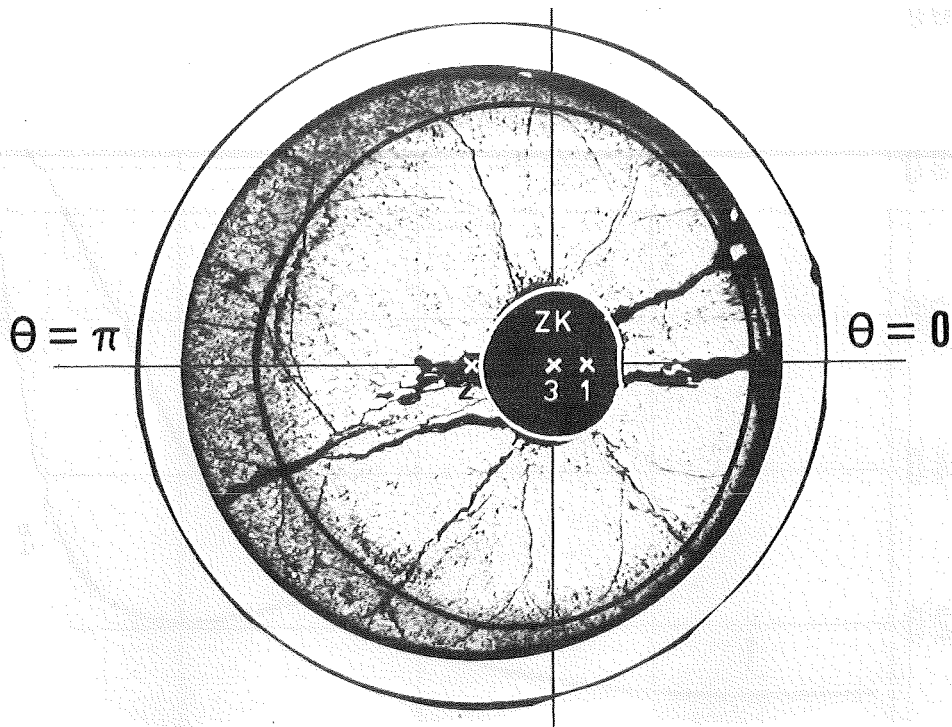


Fig. 16 Fission Gas Pressure Buildup and Release Rate: Experimental Data at Irradiation Mol-8C/Pin 8C-4



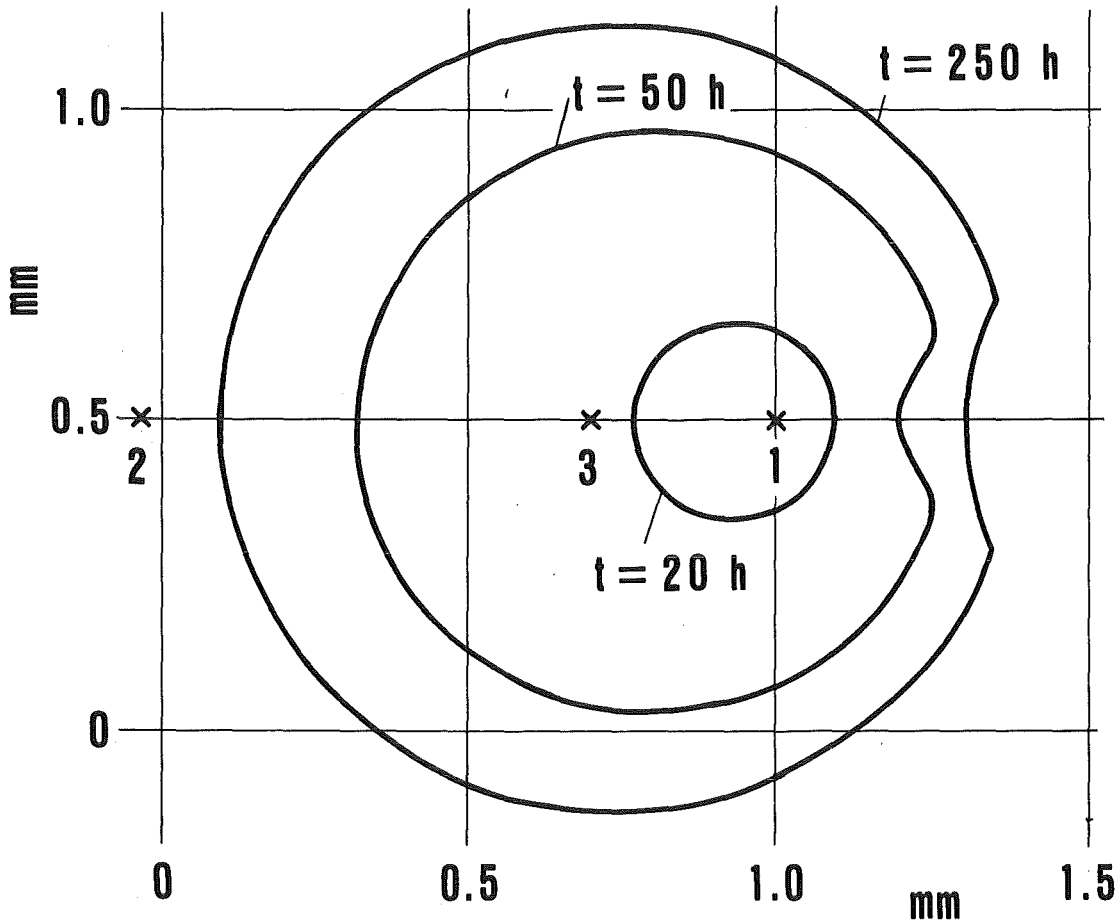
- 1 - Calculations with TRANSIENT
- 2 - Experimental Data by Microprobe Analysis

Fig. 17 Radial Distribution of Retained Fission Gas at 450 W/cm Rod Power and about 2 at % Burnup



- 1- Location of Maximum Temperature before Formation of Central Channel
- 2- Center of the Fuel Pellet
- 3- Center of the Void at the End of the Irradiation

Fig. 18 Microsection of a DUELL Pin with the Boundaries of Central Channel and the Pore Migration Zone as Calculated with TEXDIF-P



- 1- Location of Maximum Temperature before Formation of Central Channel
- 2- Center of Fuel Pellet
- 3- Center of the Void at the End of the Irradiation

Fig. 19 Central Void Formation:
Contour of the Void at Consecutive Times t